the length of the alkyl sequence in relation to that of the perfluorinated segment.

For F12Hm compounds where m = 2, 4, and 6, the structure below the transition temperature was found to consist of crystals where the molecular axes were tilted with respect to the crystal normal. Increasing the temperature effected a translation of the molecules along their axes, producing a structure where the axes were now oriented perpendicular to the surface. Either an antiparallel- or a parallel-packing structure was possible, but semiempirical energy calculations indicated that the latter was more likely. The stable structure below the transition temperature in the m = 8, 10, 12, and 14 compounds consisted of a tilted bilayer structure where the tilt angle is governed by a staggering of the CF_2 units. Above the transition temperature the molecules most likely interleave. In all cases, the mechanism by which the transition occurs was a translation of the molecules along their axes. The high-temperature structure prior to melting was found to be of a rotator phase where the molecules freely rotate about their parallel axes.

Finally, for the F12Hm compounds where $m > 14$ a different structure is evident. The diffraction results clearly indicate that the structure is more diffuse than that for the other semifluorinated alkanes. Dramatic differences in the spectroscopic, diffraction, and thermal data of these compounds support this structural change. Further work is necessary, however, in order to elucidate the precise nature of the crystal packing.

Acknowledgment. We acknowledge several helpful discussions with Professors I. Harrison (Pennsylvania State University) and E. S. Clark (University of Tennessee). We are also grateful to Grace Lim for conducting the powder diffraction experiments. This work was supported, in part, by the National Science Foundation under Grant No. DMR-8419095.

Registry No. $F12H_0$, 66563-68-6; $F12H_2$, 89109-68-2; $F12H_4$, 89109-69-3; $F12H_6$, 89109-70-6; $F12H_8$, 90499-31-3; $F12H_{10}$, 93454-72-9; $F12H_{12}$, 89109-71-7; $F12H_{14}$, 93454-73-0; $F12H_{16}$, 93454-74-1; $F12H_{18}$, 93454-75-2; $F12H_{20}$, 89109-72-8.

References and Notes

(1) Rabolt, J. F.; Russell, T. P.; Twieg, R. J. *Macromolecules* **1984**, *17*, 2786.
(2) Holz, A.; Naghizadeh, J.; Vigren, D. T. *Phys. Rev.* **1983**, *B27*, 512.
(3) Denicolo, I.; Doucet, J.; Craievich, A. F. *J. Chem. Phys.* **1983**, *78*, 1465.
(4) Doucet, J.; Denicolo, I.; Craievich, A. F.; Germain, C. *J. Chem. Phys.* **1984**, *80*, 1647.
(5) Doucet, J.; Denicolo, I.; Craievich, A. F. *J. Chem. Phys.* **1981**, *75*, 1523.
(6) Craievich, A. F.; Denicolo, I.; Doucet, J. *Phys. Rev.* **1984**, *B30*, 4782.
(7) Ungar, G. *J. Phys. Chem.* **1983**, *87*, 689.
(8) Larsson, K. *Nature (London)* **1967**, *213*, 383.
(9) Smith, A. E. *J. Chem. Phys.* **1953**, *21*, 2229.
(10) Crissman, J. M.; Passaglia, E.; Eby, R. K.; Colson, J. P. *J. Appl. Crystallogr.* **1970**, *3*, 194.
(11) Broadhurst, M. G. *J. Res. Natl. Bur. Stand. Sect. A* **1962**, *66A*, 241.
(12) Strobl, G. R. *J. Polym. Sci., Polym. Symp.* **1977**, 59, 121.
(13) Clark, E. S.; Muus, L. T. *Z. Kristallogr.* **1962**, *117*, 119.
(14) Bunn, C. W.; Howells, E. R. *Nature (London)* **1954**, *174*, 549.
(15) Bridgman, P. W. *Proc. Am. Acad. Arts Sci.* **1948**, *76*, 71.
(16) Weir, C. E. *J. Res. Natl. Bur. Stand.* **1951**, *46*, 207.
(17) Beecroft, R. I.; Swenson, C. A. *J. Appl. Phys.* **1959**, *30*, 1793.
(18) Martin, G. M.; Eby, R. K. *J. Res. Natl. Bur. Stand. Sect. A* **1968**, *A72*, 467.
(19) Hirakawa, S.; Takemura, T. *Jpn. J. Appl. Phys.* **1969**, *8*, 635.
(20) Johnson, K. W.; Rabolt, J. F. *J. Chem. Phys.* **1973**, *58*, 4536.
(21) Nakafuku, C.; Takemura, T. *Jpn. J. Appl. Phys.* **1975**, *14*, 599.
(22) Brown, R. G. *J. Chem. Phys.* **1964**, *40*, 2900.
(23) Wu, C. K.; Nicol, M. *Chem. Phys. Lett.* **1973**, *21*, 153.
(24) Campos-Vallette, M.; Rey-Lafon, M.; Lagnier, R. *Chem. Phys. Lett.* **1982**, *89*, 189.
(25) Hendra, P. J.; Jobic, H. P.; Marsden, E. P. *Spectrochim. Acta* **1977**, *A33*, 445.
(26) Barnes, J. D.; Fanconi, B. *J. Chem. Phys.* **1972**, *56*, 5190.
(27) Twieg, R. J.; Rabolt, J. F. *J. Polym. Sci., Polym. Lett. Ed.* **1983**, *21*, 901.
(28) Narang, R. S.; Sherwood, J. *Mol. Cryst. Liq. Cryst.* **1980**, *59*, 167.
(29) Snyder, R. G.; Scherer, J. R.; Gaber, B. P. *Biochem. Biophys. Acta* **1980**, *601*, 47.
(30) Farmer, B. L.; Patel, A., unpublished data.
(31) Farmer, B. L.; Eby, R. K. *Polymer* **1981**, *22*, 1487.

Kinetics of Crystallization in Semicrystalline/Amorphous Polymer Mixtures

G. C. Alfonso† and T. P. Russell*

IBM Almaden Research Center, San Jose, California 95120. *Received October 17, 1985*

ABSTRACT: The kinetics of crystallization in mixtures containing narrow molecular weight fractions of poly(ethylene oxide) (PEO) and poly(methyl methacrylate) (PMMA) have been investigated as a function of the composition and molecular weight of each component and the crystallization temperature. The radial growth rates of the spherulites have been described by a kinetic equation that incorporates the cooperative diffusion coefficient, the thickness of the crystalline lamellae, and the free energy for the formation of secondary crystal nuclei. Adjusting for an apparent molecular weight dependence of the lateral and fold surface free energies of the PEO crystals permitted the construction of a master curve from the growth rate of all the mixtures studied. A precise evaluation of the equilibrium melting point of the PEO crystals in the pure polymer and in the mixtures was hindered by annealing during crystallization and heating. This latter result casts serious doubts on the determination of an interaction parameter via a melting point depression analysis in these mixtures.

Introduction

The addition of an amorphous polymer to a semicrystalline polymer can have dramatic effects on the thermodynamic and kinetic parameters governing the crystallization. From a thermodynamic viewpoint, specific interactions in the mixture lead to a slight depression in the equilibrium melting point[1-3] and a change in the free energy for the formation of nuclei on the crystal surface.[4,5] The kinetics of crystallization are reduced by a dilution of the crystallizable component at the growth surface.[4-6] An important parameter that is modified by mixing and has significant ramifications on the overall mobility in the

†Permanent address: Istituto di Chimica Industriale, Università di Genova, 16132 Genova, Italy.

0024-9297/86/2219-1143$01.50/0

Table I
Characteristics of PEO and PMMA

M_w	M_w/M_n
PEO ($M_c \simeq 4000$)	
6 000	1.03
13 000	1.02
39 000	1.07
86 000	1.02
145 000	1.03
594 000	1.04
990 000	1.05
PMMA ($M_c \simeq 30\,000$)	
1 000	1.08
29 700	1.07
125 000	1.08
525 000	1.17

mixture is the glass transition temperature T_g.[7] Depending upon the T_g's of the pure components, this change may either enhance or retard the rate of crystal growth at a specific crystallization temperature. Finally, the molecular weights and the molecular weight distributions of the individual homopolymers can alter both the kinetics of crystallization and the thermodynamics governing mixing. Despite substantial interest in semicrystalline polymer blends, relatively few studies have appeared addressing the kinetics of the crystallization process.[6,8-15]

Most work dealing with semicrystalline/amorphous polymer mixtures has emphasized the changes produced in the morphology. Keith and Padden,[15,16] for example, noted a coarsening of the spherulitic texture as the molecular weight of the amorphous impurity was decreased. This led them to describe the spherulitic morphology in terms of a length parameter $\delta = D/G$, where D is the diffusion coefficient of the amorphous component and G is the linear growth rate of crystals. δ is effectively the distance over which noncrystallizable impurities are excluded from the growth front. This treatment, initially developed to account for the cellular growth in metallic alloys,[17,18] has been a convenient means of describing the morphology in a number of semicrystalline polymer mixtures.[16,19] However, as recently pointed out by Keith and Padden,[20] the concepts used in this treatment may be too simplistic to accurately account for the growth rate kinetics in polymeric systems.

In this work, the crystallization kinetics in semicrystalline/amorphous polymer mixtures using narrow molecular weight distribution fractions of poly(ethylene oxide) (PEO) and poly(methyl methacrylate) (PMMA) are examined. Growth rates over a wide range of molecular weights, compositions, and crystallization temperatures are presented, and an analysis is proposed that reasonably accounts for these data. In addition to this, the melting point depressions for these mixtures are discussed in terms of the evaluation of an interaction parameter. Finally, a compilation of data on the equilibrium melting point of PEO as a function of molecular weight is given and compared to predictions for the infinitely thick PEO crystal.

Experiment

All but two of the PEO specimens used in this study were the TSK Standard PEO produced by Toyo Soda Manufacturing Co., Ltd. The range of PEO molecular weights along with their corresponding polydispersities are shown in Table I. The polymers, which are calibration standards for gel permeation chromatography, were used as received without further purification. The remaining two PEO's having M_n = 6000 and 13 000, both with narrow molecular weight distributions, were obtained from Fluka Chemical Co. The characteristics of these two polymers are also shown in Table I. The PMMA used in this work were obtained from Polymer Laboratories, Ltd., with the exception of the sample with M_w = 1000, which was kindly supplied by D. J. McDonald of the Rohm and Haas Co. The characteristics of the different PMMA polymers are also given in Table I.

Mixtures of PEO and PMMA were prepared by dissolving the dried polymers in benzene at 50 °C. The solutions were quenched in a dry ice/acetone slurry and then freeze-dried in a water/ice bath for 24 h. Prior to use the mixtures were dried under vacuum at 30 °C for at least 24 h to remove traces of benzene. The dried samples were then briefly melted between aluminum foil at 140 °C under pressure to produce films 100–200 μm thick. Preparation of specimens in this manner yielded reproducible film morphologies and growth rates. Attempts were made to solution cast mixtures from chloroform as suggested by some authors.[21-23] However, regardless of the rate of solvent evaporation, nonuniform films that degraded after several heating cycles resulted. The origin of this discrepancy is unknown.

Growth rate studies were conducted on a Mettler FP85 hot stage using a Zeiss polarizing microscope equipped with a Cohu 4300 SIT television camera. For low undercoolings the crystallization rate was slow enough to follow visually with an accuracy of ±1.5 μm for each measurement during the course of sperulite growth. For high undercoolings, a temperature-jump cell comprised of two ovens independently controlled was constructed. The blend specimen was sandwiched between two cover glass slips and mounted onto an aluminum support. The cell, designed to minimize the mass of the specimen yet maintain mechanical stability, was directly mounted on the microscope stage. A thermocouple imbedded within the specimen demonstrated that ca. 15 s was necessary in order to thermally equilibrate the sample. Rapid growth rates were recorded on a video cassette, which could be played back frame-by-frame to evaluate the growth rate. Calibration of the magnification was accomplished with a standard grating micrometer. Nonlinearities in the field of view of the camera and video monitor were taken into account in the evaluation of the growth rates. Measurements of the growth rates were made by both the visual and video methods over a sufficiently large temperature range to provide ample data overlap. Good agreement was found between the two methods.

In general, the mixtures were volume filled with spherulites and, up to the impingement of the spherulites, the growth rates were found to be constant. It must be reiterated, however, that reproducible measurements of the growth rates were found only if the specimens were dried under vacuum for several hours prior to measurement. The temperatures at which the crystallizations were performed were randomly selected over the desired crystallization temperature range to prevent any systematic errors. Individual specimens were used for no more than eight different studies, at which time a fresh specimen was prepared to continue measurements.

For both pure PEO and the mixtures with PMMA measurements of the growth rate were prohibited at large undercoolings by either nonisothermal conditions or by the very high nucleation density. At high crystallization temperatures, i.e., at small undercoolings, the nucleation density was quite low. In order to avoid prohibitively long measurements, the specimens were nucleated at lower temperatures and rapidly reequilibrated at the desired crystallization temperature and measurements of the growth rate were made after a steady-state growth at this elevated temperature was established. The reliability of this procedure was verified by performing measurements in the identical manner at lower crystallization temperatures.

Melting point measurements were conducted on a Mettler FP 85 hot stage under crossed polars. At the desired crystallization temperature specimens were allowed to crystallize until a clearly discernable spherulite was evident and then heated at a rate of 3 °C/min. The melting point was taken as the temperature at which the last birefringent entity vanished. The crystallization times in these experiments were not constant due to the large range of undercoolings. In cases where the spherulites were nucleated at lower temperatures, crystallization was allowed to proceed until a discernable growth at the desired crystallization temperature was evident. During the melting, the inner seed melted well below the melting point of the crystals formed at the crystallization temperature of interest. After the disappearance of the seed nucleus melting began at the outer edges of the spherulite and proceeded in toward the center. As with mea-

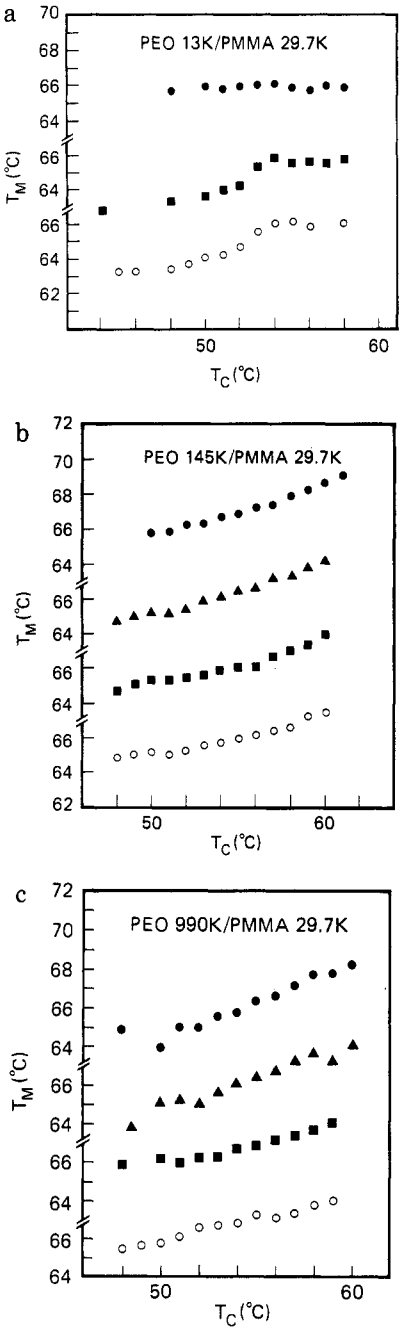

Figure 1. (a) Melting point as a function of the crystallization temperature for PEO(13 000) mixtures with PMMA(29 700). Compositions of 100% (●), 85% (■), and 70% (○) are shown. (b) Melting point as a function of the crystallization temperature for PEO(145 000) mixtures with PMMA(29 700). Compositions of 100% (●), 92.5% (▲), 85% (■), and 70% (○) are shown. (c) Melting points as a function of the crystallization temperature for PEO(990 000) with PMMA(29 700). Compositions of 100% (●), 92.5% (▲), 85% (■), and 70% (○) are shown. Note that the ordinate scales are broken.

surements at larger undercoolings, the melting point was taken as the temperature where the last birefringent entity vanished. No dependence of the melting point on the nucleation temperature was found.

Melting Point Results

Typical plots of the melting point as a function of the crystallization temperature are shown in Figure 1, parts a, b, and c, for mixtures of PMMA(29 700) with PEO(13 000) PEO(145 000) and PEO(990 000), respectively. As can be seen, the relationship between the crystallization and melting temperatures depends upon the molecular weight of the PEO and the composition of the mixture. In agreement with the results of Buckley and Kovacs,[24,25] the melting points of PEO(6000) and PEO(13 000) were independent of the crystallization temperature. For mixtures of PEO(13 000) with PMMA, however, the melting point first increased with the crystallization temperature and then at lower undercoolings was independent of the crystallization temperature. This behavior was found independent of the PMMA molecular weight. The invariance of the PEO melting point indicates that the crystals formed are either extended chain crystals or crystals with a constant number of folds. In the mixtures, the decrease in the melting point at lower crystallization temperatures may be attributed to changes in the surface free energy in the PEO crystals, an increase in the concentration of crystalline defects, or a change in the structure of the PEO crystals. Consequently these data were not used in the evaluation of T_m^0. Extrapolation of the melting points at low undercooling to the $T_m = T_c$ line were straightforward due to the invariance of T_m with T_c. The extrapolated melting point of the pure PEO(13 000) and all the mixtures was 66.0 °C. No depression in the melting point was observed to within experimental errors, indicating that the interaction parameter is zero for these mixtures.

Table II
Melting Points of Pure PEO and a Typical Mixture with PMMA

M_w PEO	M_w PMMA	wt fract PEO	$T_{m,eq}$, °C	$\Delta T_m/\Delta T_c$
6 000		1.0	64.0	0.
13 000		1.0	66.0	0.
39 000		1.0	69.0	0.28
86 000		1.0	70.4	0.28
145 000		1.0	72.1	0.30
594 000		1.0	72.7	0.31
990 000		1.0	73.3	0.38
145 000	1 000	0.85	69.9	0.27
		0.70	69.9	0.34
145 000	29 700	0.93	71.0	0.28
		0.85	69.8	0.24
		0.70	69.2	0.22
145 000	125 000	0.93	70.3	0.26
		0.85	70.5	0.28
		0.70	70.8	0.31
145 000	525 000	0.93	70.0	0.25
		0.85	69.5	0.25
		0.70	69.6	0.29

Increasing the molecular weight of the PEO dramatically altered the melting point behavior of both the pure PEO and the mixtures. For the pure PEO, the melting point continually increased with the crystallization temperature. In agreement with the results of others,[22,26] only at low undercoolings could a linear dependence of T_m on T_c be approximated. Deviations from this behavior were clearly evident at higher undercoolings. Extrapolation of these data in a manner outlined by Hoffman and Weeks[27] yielded the equilibrium melting point $T_{m,eq}$. Values of $T_{m,eq}$ for the different PEO's studied and a typical set of $T_{m,eq}$'s for one series of mixtures are given in Table II. Also listed in Table II are the slopes of the lines ($\Delta T_m/\Delta T_c$) used in the extrapolation to $T_{m,eq}$. As can be seen, $\Delta T_m/\Delta T_c$ did not remain constant but varied randomly. It cannot be assumed, however, that this reflects a change in the morphology, as suggested previously,[2] but is more likely associated with the thermal history of the specimen and the manner in which the melting point is evaluated. The values of $T_{m,eq}$ for the mixtures shown and for all the other mixtures studied exhibit a slight decrease in $T_{m,eq}$ as the concentration of PEO decreases. However, contrary to the

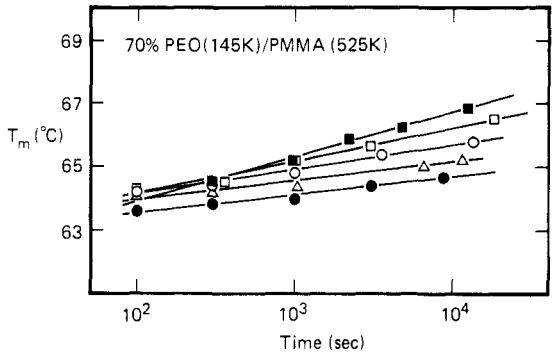

Figure 2. Melting points of 70% PEO(145 000)/30% PMMA-(525 000) mixture as a function of the time allowed for crystallization. The symbols represent crystallization temperatures of 50 °C (●); 52 °C (▲); 54 °C (○) 56 °C (□), and 58 °C (■).

results from other laboratories,[11,21,22] the dependence of $T_{m,eq}$ on concentration could not be described by a Flory–Huggins treatment. In fact, application of this treatment to these data yielded, at best, values of the interaction parameter χ equal to zero to within experimental errors.

It can be argued that the procedure used to obtain the equilibrium melting points of both PEO and its mixtures is fraught with assumptions and cannot possibly yield accurate values of $T_{m,eq}$. This argument is strengthened by the nonlinear behavior observed. Deviations from a linear behavior can result from annealing of the crystals during a crystallization process or during the heating of the specimens to melt the crystals.[28,29] A dramatic example of this former effect is shown in Figure 2, where the measured melting temperature is shown as a function of the time allowed for crystallization. Regardless of the crystallization temperature, the melting point of the PEO increased with the duration of crystallization at a rate that was dependent on the crystallization temperature. A more desirable method for obtaining $T_{m,eq}$ would be to determine the dependence of the T_m on the inverse crystal thickness, $1/L$. Extrapolation of $1/L$ to zero would then yield $T_{m,eq}$. Actually this latter method would yield the value of T_m^0, the equilibrium melting point of an infinitely thick crystal in the mixture, and would be independent of any morphological parameters. Attempts to evaluate the crystal thickness by both X-ray scattering and diffraction techniques were not successful due to the large size of the PEO crystals. With the exception of mixtures with high PEO concentrations and at large undercoolings, the characteristic long period was beyond instrumental resolution. However, even if the crystal thickness could be determined accurately, it would be necessary to measure the crystal thickness of the final crystal melting. This would necessitate the use of a time-resolved diffraction or scattering method where real time measurements could be made. Consequently, despite the deficiencies of a Hoffman–Weeks type analysis, we have utilized this method to evaluate $T_{m,eq}$. Due to the reservations stated above and to the extrapolation required in the analysis, the values of $T_{m,eq}$ reported in Table II are only to within a ±1.5 °C precision.

The values of $T_{m,eq}$ for the pure PEO should correspond to the value of T_m^0 for a given molecular weight. This was verified by comparison to previously published data. Shown in Figure 3 are the T_m^0's obtained in this study along with the existing data in the literature.[24-26,30-33] For PEO where $M_n < 40\,000$ the values of T_m^0 reported are in excellent agreement with the data of Afifi-Effat and Hay,[30] Buckley and Kovacs[24,25] and Cheng and Wunderlich.[33] The

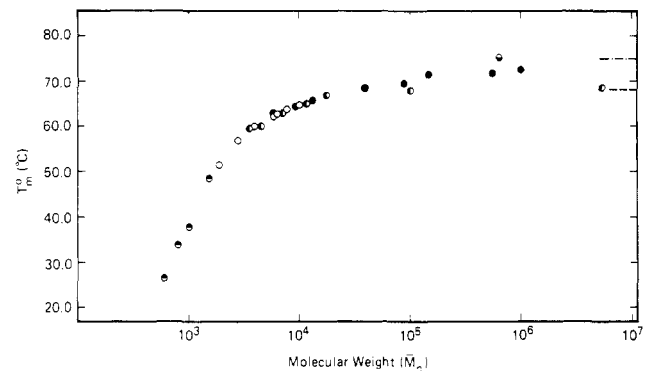

Figure 3. A compilation of the equilibrium melting point of PEO as a function of molecular weight ($\bar{M}_n$) obtained by several authors using a variety of measurement techniques. The symbols correspond to data of Hay et al.[30-32] (○); Buckley and Kovacs[24,25] (◓); Beech and Booth[26] (◒); Cheng and Wunderlich[33] (◑), and this work (●). The dashed line at ~69 °C corresponds to an extrapolation of the data of Buckley and Kovacs[24,25] to $\bar{M}_n \rightarrow \infty$, whereas the dot–dashed line corresponds to a similar extrapolation for the data of Hay.[31,32]

equilibrium melting points for the higher molecular weight PEO were found to increase continuously, in good agreement with the results of Beech and Booth[26] and Hay.[31,32] Our values of T_m^0 differ from those of Cheng and Wunderlich[33] where they observed an asymptotic behavior to ~69 °C, the value predicted by Buckley and Kovacs[24,25] for T_m^0 as $M_n \rightarrow \infty$. Extrapolation of the results reported here yield a value of $T_m^0 \simeq 76$ °C as $M_n \rightarrow \infty$, which is consistent with the results of Hay[31,32] and the surface free energy arguments of Mandelkern and Stack.[34]

Melting Point Depression

For miscible polymer mixtures where one of the components crystallizes, a depression in the melting point reflecting a change in the chemical potential of the amorphous phase due to specific interactions is expected. With the exception of PEO (13 000), a depression in the extrapolated melting point was found. As shown by Nishi and Wang,[2] for compatible polymer–polymer mixtures, the Flory–Huggins theory predicts that the equilibrium melting point of the mixture, $T_{m,eq}$ will be lower than the equilibrium melting point, T_m^0, of the pure material such that

$$\frac{1}{T_{m,eq}} = \frac{1}{T_m^0} - \frac{RV_{2u}}{\Delta h_u V_{1u}}\chi(1-\phi_2)^2 \qquad (1)$$

where R is the gas constant, Δh_u is the heat of fusion per mole of monomer, V_{iu} is the molar volume of component i with volume fraction ϕ_i, and χ is the Flory–Huggins interaction parameter. Equation 1 has been used by numerous groups to extract the value of χ from the melting point depression for the PEO/PMMA and other mixtures. However, the results shown in Table II and for the other mixtures studied are not consistent with this. Also, reformulation of eq 1 using a composition-dependent χ did not yield an equation that accurately reproduced the observed dependence of $T_{m,eq}$ upon ϕ_2.

Ideally, the melting points used in eq 1 are those of extended-chain, perfect crystals melting in a homogeneous matrix of volume fraction ϕ_2. Provided PEO and PMMA are miscible and the interlamellar region consists of a homogeneous mixture, the glass transition temperature of the amorphous phase will be higher than that predicted from the overall composition and could be quite close to the crystallization temperature. Consequently, it can be argued that, during the course of melting, the molten PEO

Table III
Parameters Used in Analysis[a]

	PEO	PMMA
Δh_u, cal/g	47.0	
b_0, Å	4.65	
M_c	4400	30 000
N_e	2200[b]	5900[b]
M_{mon}, g	44	100
V_u, cm^3 × 10^{23}	6.58	14.04
T_g, K	213.15	390
ρ, g/cm^3	1.111	1.184
C_∞	4.0	6.9
D_0, cm^2/s	6.45 × 10^7	5.87 × 10^{11}
ΔE, cal/mol	2866	5913

[a] Data in this table are found in ref 50–55. [b] Estimated from $M_c/2$.

may not have sufficient time to completely mix with the amorphous matrix and, as such, the mixture may not be at equilibrium. Therefore, the origin of the unusual composition dependence of the melting point observed in this study may be a result of a locally high concentration of PEO. In order to examine this possibility, a low molecular weight PMMA ($M_n \simeq 1000$) having a glass transition temperature of ~25 °C was studied. While end-group effects may easily alter the value of χ, the reduced glass transition temperature would alleviate problems associated with mixing. However, the composition dependence of the melting point for mixtures of PEO(145 000) and PEO(990 000) with PMMA(1000) behaved similarly. Therefore, effects associated with a nonuniform melt can be eliminated as the dominant source of the deviations.

For the PEO/PMMA mixtures studied, a maximum melting point depression of ca. 2.5 °C was observed. As stated previously, the precision to which the equilibrium melting points could be determined was ~±1.5 °C, and, as such, there may be no melting point depression in these mixtures. From eq 1 the melting point depression can be calculated if a value of χ is assumed. With the constants given in Table III and a large, negative interaction parameter ($\chi = -0.4$), a melting point depression at 60% PEO of only 4 °C is predicted. This depression, of course, diminishes with increasing χ such that at $\chi = 0$ there is no depression. Consequently, even in strongly interacting systems, the melting point depression is very small. Due to the extrapolations and assumptions necessary to obtain the $T_{m,eq}$, values of χ obtained for this system via a melting point depression analysis are questionable and any agreeement between different laboratories or with other experimental techniques can only be considered fortuitous.

It is clear that the melting point depression in the PEO/PMMA mixtures cannot be used quantitatively to evaluate the extent of mixing. The question still remains as to whether PEO and PMMA are miscible. The strongest evidence indicating the miscibility of these two polymers is some NMR relaxation time measurements in the melt[35] and the observation of a single glass transition temperature.[10,11] In the former, a single T_1 relaxation time was found, suggesting miscibility in the melt. A compilation of T_g data in the literature obtained by several techniques is shown in Figure 4. Over the entire composition range a single T_g was found, indicating compatibility. It is important to note that above 50% PEO, where the PEO crystallizes, the T_g was only weakly dependent upon composition and was quite close to that of the pure PEO. The origin of this unusual behavior may be that the transition observed dielectrically is not the true T_g of the mixture but rather a relaxation associated with the crystal/amorphous interface as proposed by Hahn et al.[36] It is worthwhile to mention that, due to the crystallization

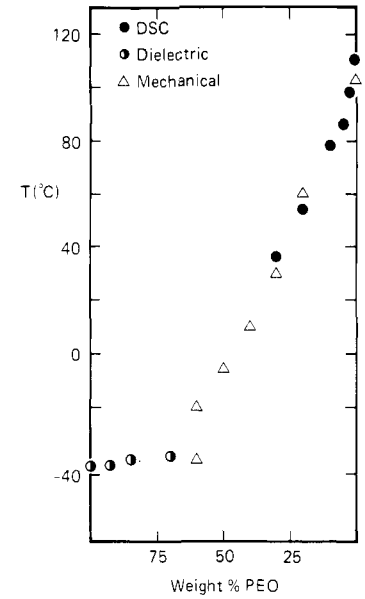

Figure 4. Glass transition temperatures of PEO/PMMA mixtures as a function of composition. The mechanical data (△) were obtained from Hoffman,[10] the DSC data (●) from Martuscelli et al.,[11] and the dielectric data (○) were measured in this laboratory.

of the PEO, the composition of the amorphous phase between the crystalline lamellae would be much richer in PMMA than the overall blend composition. A $T_g \simeq 50$–60 °C should be observed if the polymers are truly miscible. However, the melting of the PEO crystals in this temperature range prevents any quantitative assessment of a T_g. In order to address the issue of compatibility directly, small-angle neutron scattering measurements have been initiated to evaluate the χ for this mixture. In the present study it is assumed that PEO and PMMA are miscible but with a very small value of χ. Therefore, χ is assumed to be zero.

Growth Rates: Theoretical Development

Crystallization kinetics in bulk semicrystalline homopolymers have been described in the past[37,38] using a modified version of the phenomenological thery of nucleation of Turnbull and Fisher.[39,40] In this treatment, the rate of growth of the crystal, G, is governed by the work required to form a critical nucleus on the crystal surface, ΔF^*, and by the energy required to transport segments across the solid-liquid interface, ΔE. According to this theory

$$G = G^0 e^{-\Delta E/R(T-T_0)} e^{-\Delta F^*/k_B T} \quad (2)$$

where G^0 is a constant that depends upon the regime of crystallization, T_0 is the temperature at which motions necessary to transport segments across the liquid–solid interface cease, T is the temperature of crystallization, and k_B is the Boltzmann constant. This equation produces the observed bell-shaped curve for the growth rate as a function of temperature. The growth rate is nucleation controlled at low undercoolings and diffusion controlled at high undercoolings. For compatible polymer mixtures containing a noncrystallizable component, however, the process is somewhat more complex. First, the chemical potential of the liquid phase is changed due to specific interactions between the components. These interactions will alter the free energy necessary to form a critical nucleus on the crystal surface and the mobility of both the crystallizable and noncrystallizable components. Second, for crystallization to proceed, the noncrystallizable component must diffuse away from the growth front. Con-

sequently, the rate at which the growth front advances will reflect a competition between the inherent capability of the crystal to grow and the transport of the noncrystallizable component in the mixture. The slower of the two processes will dictate the kinetics. A direct ramification of this consideration is that the crystallization growth rate will depend upon the molecular weight of both components. Third, the concentration of crystallizable material at the growth front is reduced by an amount proportional to the volume fraction of the crystallizable component. Finally, the T_g of the amorphous component can alter the transport term associated with the solid–liquid interface. If the T_g of the amorphous component is higher than that of the crystalline component, then the effective value of T_0 in eq 2 will be raised, narrowing the temperature range over which crystallization can occur. If the opposite holds, then the crystallization envelope is widened.

A phenomenological equation describing the growth rate in polymer mixtures, incorporating the concepts discussed above, can be given as

$$G_m = \frac{\phi_2 k_1 k_2}{k_1 + k_2} e^{-\Delta F^*_m/k_B T_c} \tag{3}$$

where ϕ_2 is the volume fraction of the crystallizable component, T_c is the crystallization temperature, k_1 is the rate of transport of the crystallizable segments across the liquid–solid interface, k_2 is the rate at which the amorphous component can be removed from the growth front, and ΔF^*_m is the free energy of critical nucleus formation on the crystal surface modified by the presence of the amorphous component. In this form, the rate of crystal growth will depend upon the magnitudes of k_1, k_2, and ΔF^*_m. At low undercoolings, the magnitude of ΔF^*_m will be small and G_m will, therefore, be small. However, if the glass transition temperature of the mixture is high and approaches or exceeds T_m^0, then k_2 can prohibit crystallization regardless of the magnitude of ΔF^*_m. If $k_1 \gg k_2$, that is, if the transport of crystallizable material across the liquid–solid interface is fast in comparison to the rate at which the noncrystallizable material can diffuse away from the growth front, then the latter, i.e., k_2, will dominate and eq 3 reduces to

$$G_m \simeq \phi k_2 e^{-\Delta F^*_m/kT_c} \tag{4}$$

Similarly, if $k_2 \gg k_1$, then the rate of transport across the solid–liquid interface is the rate-controlling step and eq 3 reduces to

$$G_m \simeq \phi k_1 e^{-\Delta F^*_m/kT_c} \tag{5}$$

Clearly, the form of eq 3 properly bounds the crystallization growth rates. We shall now proceed to relate the different terms of eq 3 to measurable or characteristic quantities of the mixture.

Using a lattice treatment, Flory[4] and later Mandelkern[5] evaluated ΔF^* for the case of semicrystalline polymers in the presence of a low molecular weight diluent. Their treatment can be extended easily to the case of a polymer/polymer mixture such that

$$\Delta F^*_m = \frac{2b\sigma\sigma_e}{\Delta h_u f\left(1 - \frac{T}{T_m^0} - \frac{RT\chi}{\Delta h_u f}\frac{V_{2u}}{V_{1u}}(1-\phi_2)^2\right)} \tag{6}$$

where Δh_u is the heat of fusion per mole of monomer of the crystallizable component with volume fraction ϕ_2 at a temperature T, T_m^0 has been defined previously, V_{iu} is the molar volume of component i, χ is the Flory–Huggins interaction parameter, b is the thickness of the critical nucleus, and $\sigma\sigma_e$ is the product of the lateral and fold surface free energies. The temperature dependence of Δh_u is embedded in the parameter f, which is given by[27]

$$f = (2T/(T + T_m^0)) \tag{7}$$

In addition to the assumptions inherent in the initial derivation of Flory,[4] both χ and $\sigma\sigma_e$ are assumed independent of temperature and composition.

The rate of transport of segments across the liquid–solid interface should be similar to that found in the pure material except that T_0 must now be modified by the change in the glass transition temperature of the mixture. While this term deals specifically with the local mobility of the segments,[40] due to the interconnectivity of the polymer molecule, segments of the chain not crystallizing will be forced to undergo motions and, thus, will be affected by the overall mobility in the mixture. Consequently, k_1 can be written as

$$k_1 = G^0 e^{-\Delta E/R(T-T_0')} \tag{8}$$

where G^0 is a constant dependent on the regime of crystallization and is assumed equal to that of the pure semicrystalline polymer, ΔE is the energy necessary to achieve this transport, which, due to the local nature of this term, is assumed to be the same as that of the pure semicrystalline polymer, and T_0' is the value of T_0 in the mixture. T_0' may be rewritten in terms of the glass transition temperature of the mixture, T_g, and a constant C. This constant, C, has been associated with the Williams, Landel, and Ferry universal constant C_2, which has a value of 51.6 °C.[41] In this study, the value of 80.0 °C was found to best fit all the data.

The rate constant k_2 in eq 3 is related to the rate at which the amorphous component can be removed from the growth front. Let the maximum distance over which any noncrystallizable molecule must diffuse away from the growth front during crystallization be given by d. The characteristic time required for the molecule in the mixture to move this distance is given by the square of this distance divided by the diffusion coefficient D. Consequently, k_2 is

$$k_2 = d/[d^2/D] = D/d \tag{9}$$

It is evident that a center-of-mass diffusion of the amorphous component must occur in order for crystallization to proceed. At any moment, the crystal front can grow via a segmental motion of the amorphous component. However, since the center of mass of the amorphous component must be displaced by the growing crystal and since the diffusion of the amorphous and the crystallizable molecules is cooperative, then the diffusion coefficient of interest in eq 9 is the mutual diffusion coefficient $\bar{D}$. Since $\bar{D}$ is associated with center-of-mass diffusion, $\bar{D}$ is governed by the longest relaxation times of the two components in the mixture.

Kramer et al.[42] and Sillescu[43] have derived similar equations describing the mutual diffusion in a polymer mixture. With the nomenclature of Kramer

$$\bar{D} = k_B T\left[\left\{(1-\phi_2)\frac{B_1(N_e)_1}{N_1} + \phi_2\frac{B_2(N_e)_2}{N_2}\right\} \times \left(\frac{1-\phi_2}{N_1} + \frac{\phi_2}{N_2} + 2\phi_2(1-\phi_2)|\chi|\right)\right] \tag{10}$$

where $(N_e)_i$ is the entanglement molecular weight of component i with segmental mobility B_i, monomer molecular weight N_i, and volume fraction ϕ_i and χ is the Flory–Huggins interaction parameter. In the limit of $\phi_1 = 0$ one obtains the self-diffusion coefficient of component 2, namely

$$\bar{D} = k_B T B_2 (N_e)_2 / N_2^2 = D_2 \quad (11)$$

and when $\phi_2 = 0$, the self-diffusion coefficient of component 1

$$\bar{D} = k_B T B_1 (N_e)_1 / N_1^2 = D_1 \quad (12)$$

Rewriting eq 10 in terms of D_1 and D_2 yields

$$\bar{D} = \{[(1-\phi_2)N_1 D_1 + \phi_2 N_2 D_2] \times \left[\frac{1-\phi_2}{N_1} + \frac{\phi_2}{N_2} + 2\phi_2(1-\phi_2)|\chi|\right] \quad (13)$$

It should be noted that the form of eq 10–13 differs from that of Brochard and others.[44-46] To date, there is not a large enough body of data to quantitatively prove any of the existing models. The equations derived by Kramer et al[42] and Sillescu[43] were used since similar expressions for $\bar{D}$ were determined independently from two different starting points and there is some, albeit little, data available that agrees with the theoretical predictions. It would be best, however, to determine $\bar{D}$ experimentally since none of the theories incorporates the concentration dependence of the monomer friction coefficient and the interaction parameter. Experiments are in progress to evaluate $\bar{D}$ as a function of composition and temperature.

Provided the growth rate is constant on a microscopic level during the course of the crystallization, it is apparent that the growth front is exposed to a constant concentration. This prohibits a continuous exclusion and buildup of the noncrystallizable material in the direction of growth. Therefore, the amorphous component must diffuse in a direction normal to the direction of growth or into the interlamellar regions.[47,48] Consequently, the maximum distance over which any molecule would have to travel would be half of the crystal thickness or $L/2$. By substitution, eq 9 becomes

$$k_2 = 2\bar{D}/L \quad (14)$$

However, a dilemma arises in that there are two amorphous solutions (interlamellar and the bulk) with different compositions in contact with one another. Thermodynamics dictates that the system would strive to homogenize the amorphous phase. This homogenization can be prevented, however, by a variety of kinetic parameters. First, the rate of mixing will depend upon the mutual diffusion of the two components at the temperature and compositions of interest. Since the interdiffusion must occur over macroscopic size scales to fully homogenize the mixture, the times are too long in comparison to the growth rate to be feasible. In addition to this, the diffusion of the amorphous component in the interlamellar regions will be retarded due to the spatial confinement of the chains between lamellae and due to the reduced molecular mobility arising from the presence of tie chains between lamellae and loops near the lamellar surface. Also, the glass transition temperature of the interlamellar amorphous phase is critical. The closer this is to the temperature at which the crystallization occurs the slower will be any diffusion processes tending to homogenize the amorphous phase and the slower will be the crystallization because k_2 will be small.

Substitution of the different parameters into eq 3 yields

$$G_m = \frac{\phi_2 G^0 e^{-\Delta E/R(T-T_0')} 2\bar{D}/L}{G^0 e^{-\Delta E/R(T-T_0')} + 2\bar{D}/L} \exp - \frac{2b\sigma\sigma_e}{k_B T \Delta h_u f\left(1 - T/T_m^0 - \frac{RT}{\Delta h_u f}\frac{V_{2u}}{V_{1u}}\chi(1-\phi_2)^2\right)} \quad (15)$$

This can be rewritten as

$$\alpha = -\sigma\sigma_e\beta \quad (16)$$

where

$$\alpha = \ln G_m - \ln \phi_2 - \ln G^0 + (\Delta E/R(T - T_0')) + \ln\left(1 + \frac{G^0 L e^{-\Delta E/R(T-T_0')}}{2\bar{D}}\right) \quad (17)$$

and

$$\beta = \left(\frac{2b}{k_B T}\right)\left[(\Delta h_u f \Delta T/T_m^0) - \frac{RTV_{2u}}{V_{1u}}\chi(1-\phi_2)^2\right]^{-1} \quad (18)$$

Thus, parameters associated with kinetic processes are contained in α, whereas the thermodynamic variables are isolated in β. If the product of the surface free energies is independent of composition and temperature, then, according to eq 16, for a given molecular weight of PEO, all the growth rate data regardless of the composition and molecular weight of the amorphous component should produce a single straight line when α is plotted against β.

It is important to examine eq 15 in the absence of a polymer diluent. In this limit $\phi_2 = 1$ and $\bar{D}_2 = D_2$ and we get

$$G_m = \frac{G^0 e^{-\Delta E/R(T-T_0)} 2D_2/L}{G^0 e^{-\Delta E/R(T-T_0)} + 2D_2/L} \exp\{-2b\sigma\sigma_e/k_B T \Delta h_u f(1 - T/T_m^0)\} \quad (19)$$

Provided that the crystallization temperature is not too close to T_0, $2D_2/L$ will dominate the denominator and eq 19 reduces to eq 2, the growth rate equation for a semicrystalline homopolymer, as it must.

In eq 15 and 17 the ratio of $\bar{D}/G$ appears, which is a modified version of the Keith–Padden δ parameter, incorporating the cooperative diffusion coefficient. However, it is this length defined by δ in comparison to the thickness of the crystalline lamellae that is critical for the consideration of the growth rates in compatible polymer mixtures. It is important reemphasize that eq 15 was developed for mixtures where the growth rate is constant on a microscopic level, which, in turn, necessitates the incorporation of the noncrystalline component in the interlamellar regions.

Growth Rates: Experimental Results

Typical isothermal growth rate curves as a function of the crystallization temperature are shown in Figure 5 for mixtures of PEO(990 000) with the indicated molecular weights and concentrations of PMMA. Similar behavior was found for the different PEO molecular weights. As mentioned previously, all growth rates reported were constant up to the point of spherulite impingement. No systematic change in the spherulitic texture was observed with the exception of some 55% PEO mixtures at low undercoolings where the spherulitic texture was too coarse to accurately evaluate the growth rates.

The data in Figure 5 contain several interesting features. First, no maxima in the growth rate curves were found. This result is very surprising for the lower PEO concentrations since the glass transition temperatures of the homogeneous mixtures are ca. 0 °C, which is only 15 °C below the lowest experimental temperature. Reliable measurements could not be obtained at higher undercoolings due to the increase in the nucleation density and/or nonisothermal conditions of crystallization. Second, as the concentration of PEO decreased, the rate of

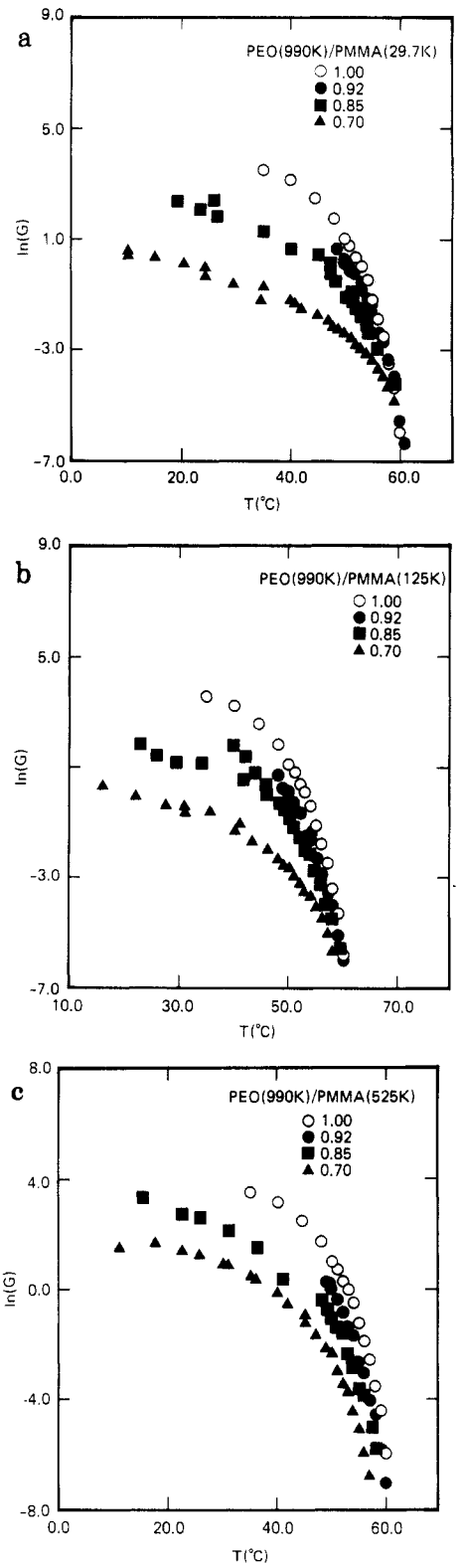

Figure 5. (a) Natural logarithm of the linear growth rates (μm/min) for mixtures of PEO(990 00) with PMMA(29 700) as a function of the temperature of crystallization. (b) Natural logarithm of the linear growth rates (μm/min) for mixtures of PEO(990 000) with PMMA(125 000) as a function of the crystallization temperature. (c) Natural logarithm of the linear growth rates (μm/min) for mixtures of PEO(990 000) with PMMA(525 000) as a function of the crystallization temperature. The different compositions are indicated in the legends.

crystallization decreased. This decrease was not constant over the entire temperature range studied and depended on the molecular weight of the PMMA. The separation in the growth rate curves at lower undercoolings increased

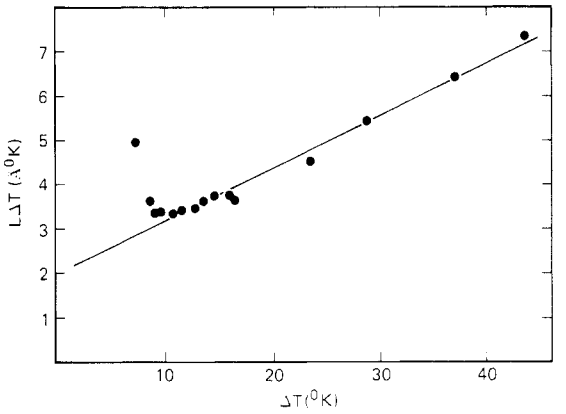

Figure 6. The product of the crystal thickness (L) and the undercooling ($\Delta T = T_c - T_m^0$) as a function of the undercooling. Solid points are from Skoulios et al.[48]

as the molecular weight of the PMMA increased. Finally, the growth rates became imperceptibly small some 8–10 °C below the equilibrium melting point. This latter feature is not unusual, but continuation of the data in Figure 5 would indicate that the growth rates would merge well below the equilibrium melting point. This behavior would not be expected if the melting points were depressed significantly.

The growth rate data for all the mixtures were analyzed in accordance with eq 16. Use of this analysis requires values of L, $\bar{D}$, χ, ΔE, and T_0'. Skoulios and co-workers[49] have examined the dependence of the PEO crystal thickness on temperature. Assuming that L varies inversely with the undercooling ΔT, their data were plotted as $L\Delta T$ vs. ΔT in Figure 6. As can be seen, over the range of undercoolings of interest here (>8 K), the data fall on a straight line with a slope, equivalent to a limiting crystal thickness at large ΔT, of 116 Å and an intercept of 2037 Å K. Measurements in this laboratory at large undercoolings are in agreement with their results. Values of $\bar{D}$ were calculated from eq 13 with data available in the literature.[50-55] The parameters used in these calculations are given in Table III and, as stated previously, χ was assumed equal to zero. The magnitude of ΔE used in calculations for the mixtures was identical with that used in the pure PEO. T_0' was assumed to be given by the glass transition temperature of the mixture T_g plus a constant C. T_g for the mixture was calculated from the Fox relationship,[56] and C was determined from the growth rate data of the pure PEO such that a plot of α vs. β yielded a straight line. The value of C was kept constant for a given molecular weight of PEO.

Plots of α vs. β are shown in Figure 7 for mixtures of PEO(145 000) with the three different molecular weights of PMMA indicated. Similar results were obtained for the different molecular weights of PEO studied. As can be seen, the data superpose, indicating that eq 16 reasonably accounts for the dependence of the growth rate on composition with the exception of the PMMA(29 700) mixtures. Discrepancies at low undercoolings were observed for all the PMMA(29 700) mixtures irrespective of the molecular weight of PEO used. The origin of these deviations is not known at present, but it is interesting to note that this molecular weight corresponds to the critical molecular weight for entanglement coupling of PMMA of $M_w = 31\,500$.[50]

Equation 16, however, predicts that α varies linearly with β. As can be seen from these data, significant curvature is observed. This may be suggesting that $\sigma\sigma_e$ is increasing with decreasing temperature. Whether this

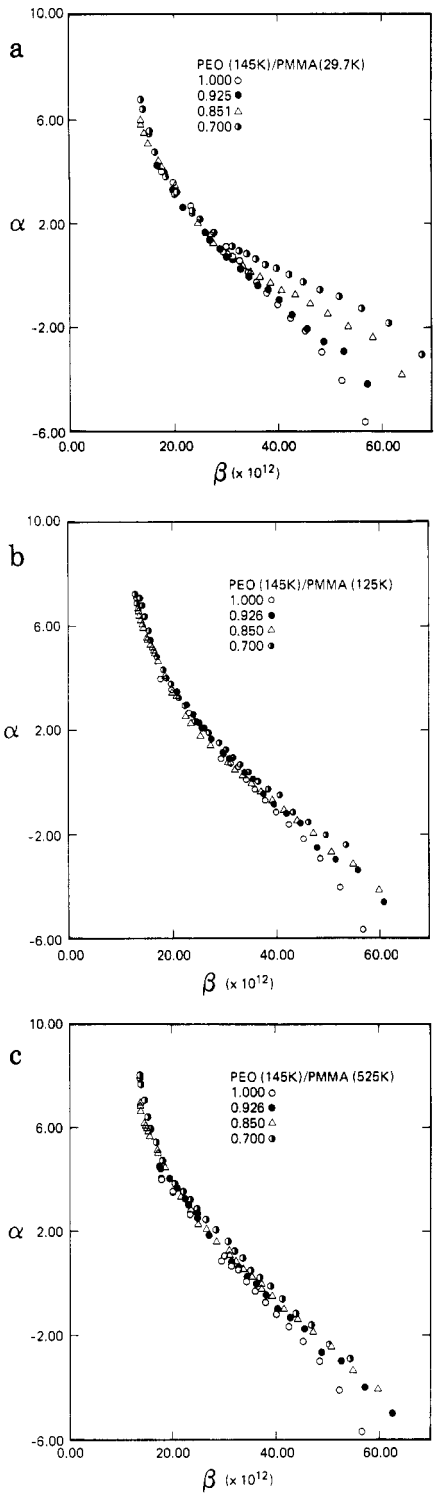

Figure 7. (a) The kinetic parameter α (dimensionless) as a function of the thermodynamic parameter β (units of cm/g·cal^2) for mixtures of PEO(143 000) with PMMA(29 700). The different compositions are indicated in the legend. (b) The kinetic parameter α (dimensionless) as a function of the thermodynamic parameter β (units of cm/(g·cal^2)) for mixtures of PEO(145 000) with PMMA(125 000). (c) The kinetic parameter α (dimensionless) as a function of the thermodynamic parameter β (units of cm/(g·cal^2)) for mixtures of PEO(145 000) with PMMA(525 000).

variation corresponds to the different growth rate regimes as discussed by Hoffman et al.[38] is now known. It should be noted that plots of α vs. β for the pure PEO were linear and that the curvature observed stems from the growth rate data of the mixtures.

Superposing the data for the different molecular weight PMMA mixtures (with the exception of the PMMA-

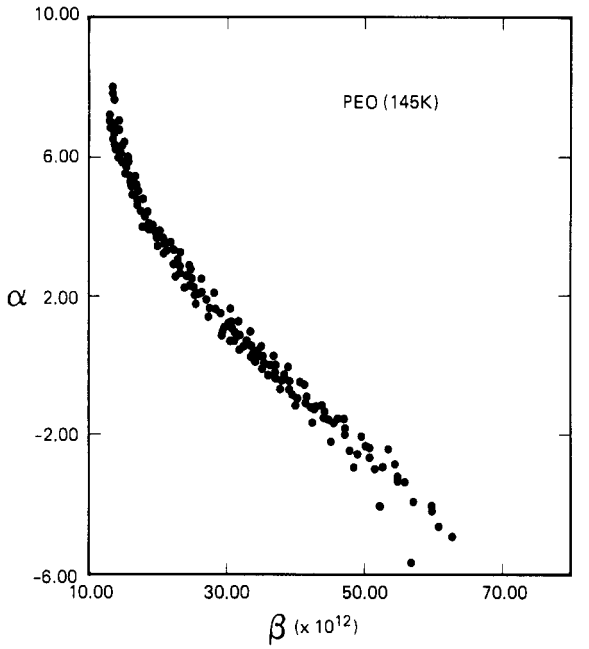

Figure 8. Composite diagram of α vs. β for mixtures of PEO(145 000) with PMMA(125 000) and PMMA(525 000).

Table IV
Growth Rate Data for Pure PEO

M_w	$G^0 \times 10^{-5}$, cm/s	$\sigma\sigma_e$, (erg/cm^2)^2
13 000	3.6	363
145 000	2.2	496
594 000	8.0	627
990 000	48.3	724

(29 700)) is shown in Figure 8. It is clear from this plot that eq 16 accurately accounts for the effect of the molecular weight of the noncrystallizable component provided it is larger than the critical molecular weight. In order to compare the data for the different molecular weights of PEO the data must be normalized according to G_0 and $\sigma\sigma_e$ for each PEO. As mentioned, plots of α vs. β for the pure PEO were linear, yielding the values of G_0 and $\sigma\sigma_e$ shown in Table IV. Normalizing all the data to that of PEO(145 000) resulted in the composite plot of α vs. β shown in Figure 9. Given the wide range of molecular weights of both components, the large composition range, and the simplicity of eq 16, the agreement between the different data sets is remarkably good. In fact, most of the scatter evident in Figure 9 originated in two different data sets. Considering the number of different experiments and the amount of data that is contained in this composite diagram, the proposed growth rate equation, despite the assumptions made, appears to describe the experimental data quite well.

While the proposed growth rate equation cannot fully account for the complex process of crystallization in semicrystalline/amorphous polymer mixtures, it is evident that this equation incorporates the most critical parameters in the proper manner. Accurate experimental evaluation of χ and $\bar{D}$ for the different molecular weights and compositions of PEO and PMMA over the temperature intervals studied here may improve the superpositioning of the data.

Conclusions

A systematic study on the crystallization and melting of a series of narrow molecular weight fractions of PEO and PMMA has been performed over a wide range of molecular weights, compositions, and crystallization temperatures. A phenomenological equation has been pro-

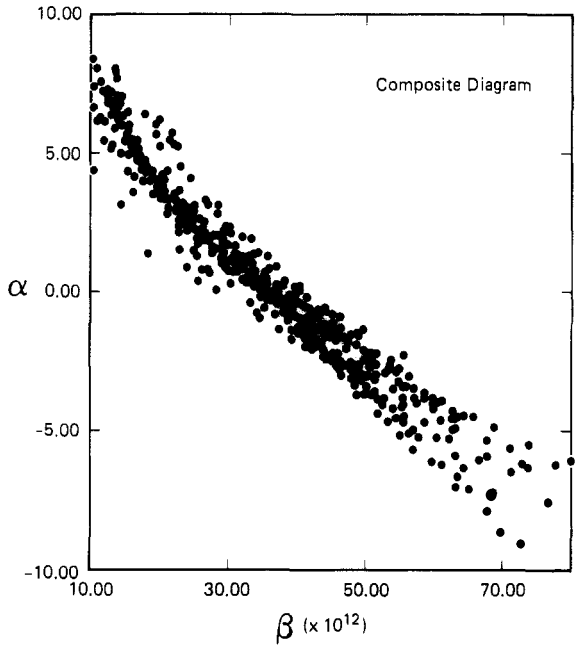

Figure 9. Composite diagram of α vs. β for all the PEO and PMMA mixtures studied (over 40 in all). No distinctions have been made for the different mixtures due to the density of points. Units are the same as in Figure 7. The data for the different molecular weights of PEO have been normalized to the data of PEO where $\bar{M}_n$ = 145 000, taking into account the values of $\sigma\sigma_e$ and G_0 given in Table IV.

posed incorporating the linear growth rate, cooperative diffusion coefficient, lamellar thickness, and the critical free energy of secondary crystal nucleus formation. This treatment was found to describe the observed growth rates quite well. Deviations were found when the molecular weight of the amorphous component was approximately equal to the critical molecular weight for entanglement coupling.

In addition it has been found that evaluation of the Flory–Huggins interaction parameter via melting point depression analysis was not possible. Crystal annealing at the crystallization temperature or during heating prohibited a precise evaluation of the equilibrium melting point. While we have investigated only one polymer pair, in general, the accuracy to which the equilibrium melting point can be determined is comparable to the depression in the melting point due to specific interactions and casts serious doubts on the evaluation of the interaction parameter via this method. Finally, the equilibrium melting points of the pure PEO, for M_w < 40 000, were in excellent agreement with previously existing data. At very high molecular weights, the values of the melting point were slightly lower than that suggested by Hay[31,32] and Mandelkern[34] but were higher than the previous extrapolation of Kovacs,[24] and recent results of Cheng and Wunderlich.[33]

Acknowledgment. We thank Dr. H. D. Keith of AT&T Bell Laboratories for his comments and helpful suggestions on this work.

References and Notes

(1) Flory, P. J. *Principles of Polymer Chemistry*; Cornell University: Ithaca, NY, 1953.
(2) Nishi, T.; Wang, T. T. *Macromolecules* **1975**, *8*, 909.
(3) Rim, P. B.; Runt, J. P. *Macromolecules* **1984**, *17*, 1520.
(4) Flory, P. J. *J. Chem. Phys.* **1949**, *17*, 223.
(5) Mandelkern, L. *J. Appl. Phys.* **1955**, *26*, 443.
(6) Boon, J.; Azcue, J. M. *J. Polym. Sci., Polym. Phys. Ed.* **1968**, *6*, 885.
(7) Paul, D. R., Newman, S., Eds. *Polymer Blends*; Academic: New York, 1978; Vol. 1 and 2.
(8) Ong, C. J.; Price, F. P. *Polym. Sci., Polym. Symp.*, **1978**, *No. 63*, 59; **1969**, *No. 2*, 207.
(9) Yeh, G. S. Y.; Lambert, S. L. *J. Polym. Sci., Part A-2* **1972**, *10*, 1183.
(10) Hoffman, D. M., Ph.D. Thesis, University of Massachusetts, Amherst, MA, 1979.
(11) Martuscelli, E.; Pracella, M.; Yue, W. P. *Polymer* **1984**, *25*, 1097.
(12) Calahorra, E.; Cortazar, M.; Guzman, G. M. *Polymer* **1982**, *23*, 1322.
(13) Wang, T. T.; Nishi, T. *Macromolecules* **1977**, *10*, 421.
(14) Gornick, F.; Mandelkern, L. *J. Appl. Phys.* **1962**, *33*, 907.
(15) Keith, H. D.; Padden, F. J. *J. Appl. Phys.* **1964**, *35*, 1270, 1286.
(16) Keith, D. H.; Padden, F. J. *J. Appl. Phys.* **1963**, *34*, 2409.
(17) Rutter, J. W.; Chalmers, B. *Can. J. Phys.* **1953**, *31*, 51.
(18) Tiller, W. A.; Rutter, J. W. *Can. J. Phys.* **1956**, *34*, 96.
(19) Warner, F. P.; MacKnight, W. J.; Stein, R. S. *J. Polym. Sci., Polym. Phys. Ed.* **1977**, *15*, 2113.
(20) Keith, D. H.; Padden, P. J. *Bull. Am. Phys. Soc.* **1984**, *29*, 452.
(21) Cortazar, M. M.; Calahorra, M. F. Guzman, G. M. *Eur. Polym. J.* **1982**, *18*, 165.
(22) Martuscelli, E.; Demma, G. B. *Polymer Blends: Processing, Morphology and Properties*; Martuscelli, E., Palumbo, R., Kryszewski, M., Eds.; Plenum: New York, 1979; p 101.
(23) Li, X.; Hsu, S. L. *J. Polym. Sci., Polym. Phys. Ed.* **1984**, *22*, 1331.
(24) Buckley, C. P.; Kovacs, A. J. *Prog. Colloid. Polym. Sci.* **1975**, *58*, 44.
(25) Buckley, C. P.; Kovacs, A. J. *Colloid. Polym. Sci.* **1976**, *254*, 695.
(26) Beech, D. R.; Booth, C. *J. Polym. Sci., Polym. Lett. Ed.* **1970**, *8*, 731.
(27) Hoffman, J. D.; Weeks, J. J. *J. Chem. Phys.* **1962**, *37*, 1723.
(28) Alfonso, G. C.; Pedemonte, E.; Ponzetti, L. *Polymer* **1979**, *20*, 104.
(29) Weeks, J. J. *J. Res. Nat. Bur. Stand., Sect. A* **1963**, *67A*, 441.
(30) Afifi-Effat, A. M.; Hay, J. N. *J. Chem. Soc., Faraday Trans. 2* **1972**, *68*, 656.
(31) Hay, J. N. *J. Polym. Sci., Polym. Chem. Ed.* **1976**, *14*, 2845.
(32) Hay, J. N. *Makomol. Chem.* **1976**, *162*, 63.
(33) Cheng, S. Z.; Wunderlich, B., in preparation.
(34) Mandelkern, L.; Stack, G. M. *Macromolecules* **1984**, *17*, 871.
(35) Martuscelli, E.; Demma, G.; Rossi, E.; Segre, A. L. *Polym. Commun.* **1983**, *24*, 266.
(36) Hahn, B.; Wendorff, J.; Yoon, D. Y. *Macromolecules* **1985**, *18*, 718.
(37) Mandelkern, L.; Quinn, F. A.; Flory, P. J. *J. Appl. Phys.* **1954**, *25*, 830.
(38) Hoffman, J. D.; Davis, G. T.; Lauritzen, J. I. *Treatise on Solid State Chemistry*; Hannay, N. B., Ed.; Plenum: New York, 1976; Vol. 3, Chapter 7.
(39) Turnbull, D.; Fischer, J. C. *J. Chem. Phys.* **1949**, *17*, 71.
(40) Lauritzen, J. I.; Hoffman, J. D. *J. Appl. Phys.* **1973**, *44*, 4340.
(41) Williams, M. C.; Landel, R. F.; Ferry, J. D. *J. Am. Chem. Soc.* **1955**, *77*, 3701.
(42) Kramer, E. J.; Green, P.; Palmstrom, C. J. *Polymer* **1984**, *25*, 473.
(43) Sillescu, H. *Makromol. Chem., Rapid Commun.* **1984**, *5*, 519.
(44) Brochard, F.; Jouffroy, J.; Levinson, P. *Macromolecules* **1983**, *16*, 1638; **1984**, *17*, 2925.
(45) de Gennes, P.-G. *J. Chem. Phys.* **1980**, *72*, 4756.
(46) Binder, K. *J. Chem. Phys.* **1983**, *79*, 6387.
(47) Russell, T. P.; Stein, R. S. *J. Polym. Sci., Polym. Phys. Ed.* **1983**, *21*, 999.
(48) Morra, B. S., Ph.D. Thesis, University of Massachusetts, Amherst, MA, 1980.
(49) Arlie, J. P.; Spegt, P.; Skoulios, A. *Makromol. Chem.* **1967**, *104*, 212.
(50) Ferry, J. D. *Viscoelastic Properties of Polymers*, 3rd ed.; Interprises: New York, 1980.
(51) Flory, P. J. *Statistical Mechanics of Chain Molecules*; Wiley: New York, 1969.
(52) Brandrup, J., Immergut, E. H., Eds. *Polymer Handbook*: Wiley Interscience: New York, 1975.
(53) Van Krevelen, D. W. *Properties of Polymers*; Elsevier: Amsterdam, 1976.
(54) Takahashi, Y.; Sumita, I.; Tadokoro, H. *J. Polym. Sci., Polym. Phys. Ed.* **1973**, *11*, 2113.
(55) Wunderlich, B. *Macromolecular Physics: Crystal Nucleation, Growth, Annealing*; Academic: New York, 1976; Vol. 2.
(56) Fox, T. G. *Bull. Am. Phys. Soc.* **1956**, *1*, 123.